Feasibility of terahertz lasing in optically pumped epitaxial multiple graphene layer structures

V. Ryzhii,[1,2,a)] M. Ryzhii,[1,2] A. Satou,[1,2,b)] T. Otsuji,[2,3] A. A. Dubinov,[4] and V. Ya. Aleshkin[4]
[1]*Computational Nanoelectronics Laboratory, University of Aizu, Aizu-Wakamatsu 965-8580, Japan*
[2]*Japan Science and Technology Agency, CREST, Tokyo 107-0075, Japan*
[3]*Research Institute of Electrical Communication, Tohoku University, Sendai 980-8577, Japan*
[4]*Institute for Physics of Microstructures, Russian Academy of Sciences, Nizhny Novgorod 603950, Russia*

(Received 18 August 2009; accepted 14 September 2009; published online 22 October 2009)

A multiple graphene layer (MGL) structure with a stack of GLs and a highly conducting bottom GL on SiC substrate pumped by optical radiation is considered as an active region of terahertz and far infrared lasers with external metal mirrors. The dynamic conductivity of the MGL structure is calculated as a function of the signal frequency, the number of GLs, and the optical pumping intensity. The utilization of optically pumped MGL structures might provide the achievement of lasing with the frequencies of about 1 THz at room temperature due to a high efficiency of pumping. © *2009 American Institute of Physics*. [doi:10.1063/1.3247541]

I. INTRODUCTION

Since the first experimental demonstrations of the nontrivial properties of graphene (see, for instance, Refs. 1 and 2 and numerous subsequent publications), due to the gapless energy spectrum of graphene, the latter can be used as an active region in the terahertz and far infrared (FIR) lasers with optical or injection pumping.[3,4] The optical pumping with the photon energy $\hbar\Omega$ leads to the generation of electrons and holes with the energy $\varepsilon_0=\hbar\Omega/2$. Since the interaction of electrons and holes with optical phonons is characterized by the fairly short time τ_0, the photogenerated electrons and holes quickly emit cascades of N optical phonons, where $N=[\varepsilon_0/\hbar\omega_0]$ and $[X]$ means the integer part of X. Due to relatively high energy of optical phonons in graphene ($\hbar\omega_0 \simeq 200$ meV), the number N can vary from zero (pumping by CO_2 lasers) to a few units (pumping by quantum cascade lasers or semiconductor injection diode lasers). Thus, the photogenerated electrons and holes populate the low energy regions of the conduction and valence bands of graphene[3] (see also Refs. 5 and 6). As a result, the Fermi levels of electrons and holes are separated and shifted from the Dirac point to the conduction and valence bands, respectively. This corresponds to the population inversion for the interband transitions with absorption or emission of photons with relatively low energies $\hbar\omega<2\varepsilon_F$, where ε_F is the quasi-Fermi energy of the electron and hole distributions, and leads to the negative contribution of the interband transitions to the real part of the dynamic conductivity Re σ_ω (which includes the contributions of both interband and intraband transitions). If Re $\sigma_\omega<0$, the stimulated emission of photons with the relatively low energy $\hbar\omega$ (in the terahertz or FIR range) is possible. The intraband contribution is primarily associated with the Drude mechanism of the photon absorption. As shown previously, the realization of the condition of lasing is feasible.[3,6] Some possible schemes of the graphene lasers (with metal waveguide structure or external metal mirrors) utilizing the above mechanism of optical pumping were considered recently (see, for instance, Ref. 7).

In particular, the laser structure evaluated in Ref. 7 includes two graphene layers. Relatively weak absorption of optical radiation with the efficiency per each layer $\beta=\pi e^2/\hbar c\simeq 0.023$, where e is the electron charge, $\hbar$ is the reduced Planck constant, and c is the speed of light, necessitates the use of rather strong optical pumping. This drawback can be eliminated in the structures with multiple graphene layers (MGLs). Such epitaxial MGL structures including up to 100 very perfect graphene layers with a high electron mobility ($\mu\simeq 250\,000$ cm^2/s V) preserving up to the room temperatures and, hence, with a long momentum relaxation time were recently fabricated using the thermal decomposition from a 4*H*-SiC substrate.[8,9] The incident optical radiation can be almost totally absorbed in these MGL structures providing enhanced pumping efficiency. A long momentum relaxation time (up to 20 ps)[10] implies that the intraband (Drude) absorption in the terahertz and FIR ranges can be weak. The optically pumped MGL structures in question with the momentum relaxation time about several picoseconds at room temperature might be ideal active media for interband terahertz lasers. The situation, however, is complicated by the presence of highly conducting bottom GL (and, hence, absorbing terahertz and FIR radiation due to the intraband processes) near the interface with SiC as a result of charge transfer from SiC.

In this paper, we analyze the operation of terahertz lasers utilizing optically pumped MGL structures by calculating their characteristics as function of the number of graphene layers K and optical pumping intensity I_Ω and demonstrate the feasibility of realization of such lasers operating at the frequencies from about 1 THz to several terahertz at room temperatures.

[a)]Electronic mail: v-ryzhii@u-aizu.ac.jp.
[b)]Electronic mail: a-satou@u-aizu.ac.jp.

II. MODEL

We consider a laser structure with an MGL structure on a SiC substrate serving as its active region. Although the active media under consideration can be supplemented by different resonant cavities, for definiteness we address the MGL structure placed between the highly reflecting metal mirrors (made of Al, Au, or Ag) as shown in Fig. 1(a). It is assumed that the MGL structure under consideration comprises K upper GLs (to which we refer to just as GLs) and a highly conducting bottom layer with a Fermi energy of electrons ε_F^B, which is rather large: $\varepsilon_F^B \simeq 400$ meV.[8] Apart from this, we briefly compare the MGL structure in question with that in which the bottom GL is absent. The latter structure can be fabricated by an additional peeling of upper GLs and depositing them on a Si substrate.

Due to the photogeneration of electrons and holes with the energy $\varepsilon_0=\hbar\Omega/2$, followed by their cooling associated with the cascade emission of optical phonons, low energy states near the bottom of the conduction band and the top of the valence band can be essentially occupied. Taking into account that elevated electron and hole densities (at elevated temperatures and sufficiently strong optical pumping considered in the following), the electron and hole distributions in the range of energies $\varepsilon \ll \hbar\omega_0$ in the kth graphene layer ($1 \leq k \leq K$) can be described by the Fermi functions with the quasi-Fermi energies $\varepsilon_F^{(k)}$ [see Fig. 1(b)]. The case of relatively weak pair collisions of the photogenerated electrons and holes (due to their low densities) in which the energy distributions deviate from the Fermi distributions was studied in Ref. 6. Using the Falkovsky–Varlamov formula[11] for the dynamic conductivity of a MGL structure generalized for nonequilibrium electron-hole systems,[3] one can obtain

$$\mathrm{Re}\,\sigma_\omega^B = \left(\frac{e^2}{4\hbar}\right)\left\{1-\left[1+\exp\left(\frac{\hbar\omega/2-\varepsilon_F^B}{k_BT}\right)\right]^{-1} - \left[1+\exp\left(\frac{\hbar\omega/2+\varepsilon_F^B}{k_BT}\right)\right]^{-1}\right\} + \left(\frac{e^2}{4\hbar}\right)\frac{4k_BT\tau_B}{\pi\hbar(1+\omega^2\tau_B^2)}\ln\left[1+\exp\left(\frac{\varepsilon_F^B}{k_BT}\right)\right] \quad (1)$$

for the bottom GL and

$$\mathrm{Re}\,\sigma_\omega^{(k)} = \left(\frac{e^2}{4\hbar}\right)\tanh\left(\frac{\hbar\omega-2\varepsilon_F^{(k)}}{4k_BT}\right) + \left(\frac{e^2}{4\hbar}\right)\frac{8k_BT\tau}{\pi\hbar(1+\omega^2\tau^2)}\ln\left[1+\exp\left(\frac{\varepsilon_F^{(k)}}{k_BT}\right)\right] \quad (2)$$

for the GLs with $1 \leq k \leq K$. Here τ_B and τ are the electron and hole momentum relaxation times in the bottom and other GLs, respectively, T is the electron and hole temperature, and k_B is the Boltzmann constant. The first and second terms in the right-hand sides of Eqs. (1) and (2) correspond to the interband and intraband transitions, respectively, which are schematically shown by arrows in Fig. 1(b). For simplicity we shall disregard the variation in the electron and hole densities in the bottom GL under the optical pumping, so that the electron-hole system in this GL is assumed to be close to equilibrium with the Fermi energy ε_F^B determined by the interaction with the SiC substrate.

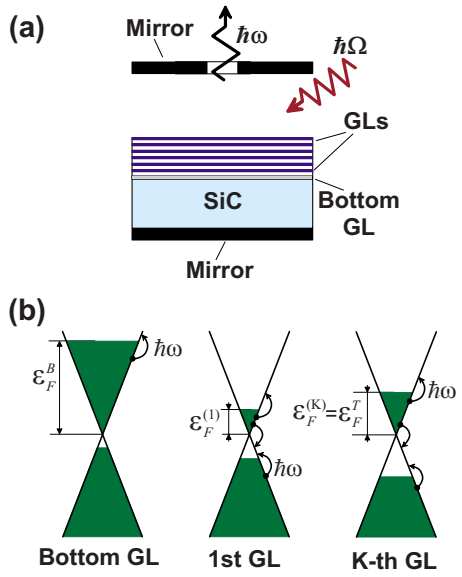

FIG. 1. (Color online) (a) Schematic view of a laser with a MGL structure. (b) Occupied (by electrons) and vacant states in different GLs under optical pumping. Arrows show transitions related to interband emission and intraband absorption of THz photons with energy $\hbar\omega$ (interband transitions related to optical pumping as well the processes of intraband relaxation of the photogenerated electrons and holes are not shown).

The quasi-Fermi energies in the GLs with $k \geq 1$ are mainly determined by the electron (hole) density in this layer Σ_k, i.e., $\varepsilon_F^{(k)} \propto \sqrt{\Sigma^{(k)}}$ and, therefore, by the rate of photogeneration $G_\Omega^{(k)}$ by the optical radiation (incident and reflected from the mirror) at the kth GL plane. Using Eq. (2) for $\hbar\omega = \hbar\Omega$, we obtain

$$G_\Omega^{(k)} = \frac{I_\Omega^{(k)}}{\hbar\Omega}\left(\frac{\pi e^2}{\hbar c}\right)\tanh\left(\frac{\hbar\Omega-2\varepsilon_F^{(k)}}{4k_BT}\right). \quad (3)$$

Here, $I_\Omega^{(k)}$ is the intensity (power density) of the optical pumping radiation at the kth GL. At $\hbar\Omega > 2\varepsilon_F^{(k)}$ (for all GLs), Eq. (3) yields $G_\Omega^{(k)} \simeq \beta I_\Omega^{(k)}/\hbar\Omega$. Considering the attenuation of the optical pumping radiation due to its absorption in each GL, one can obtain

$$G_\Omega^{(k)} = \frac{I_\Omega}{\hbar\Omega}\beta[(1-\beta)^{K-k} + (1-\beta_B)^2(1-\beta)^{K+k-1}]. \quad (4)$$

Here I_Ω is the intensity of incident pumping radiation and $\beta_B = (4\pi/c)\sigma_\Omega^B$. The latter quantity accounts for the absorption of optical pumping radiation in the bottom layer.

A relationship between $\varepsilon_F^{(k)}$ and $G_\Omega^{(k)}$ is determined by the recombination mechanisms. We assume that $\varepsilon_F^{(k)} \propto [G_\Omega^{(k)}]^\gamma$, where γ is a phenomenological parameter. In this case,

$$\varepsilon_F^{(k)} = \varepsilon_F^B\left[(1-\beta)^{K-k}\frac{1+(1-\beta_B)^2(1-\beta)^{2k-1}}{1+(1-\beta_B)^2(1-\beta)^{2K-1}}\right]^\gamma, \quad (5)$$

where $\varepsilon_F^B = \varepsilon_F^{(K)}$ is the quasi-Fermi energy in the topmost GL.

III. MGL STRUCTURE NET DYNAMIC CONDUCTIVITY

Taking into account that the thickness of the MGL structure is small in comparison with the wavelength of terahertz/FIR radiation, the generation and absorption of the latter is determined by the real part of the net dynamic conductivity

$$\mathrm{Re}\ \sigma_\omega = \mathrm{Re}\ \sigma_\omega^B + \mathrm{Re}\sum_{k=1}^{K} \sigma_\omega^{(k)}. \tag{6}$$

Taking into account that in the frequency range under consideration $\hbar\omega \ll \varepsilon_F^B$, so that one can neglect the first term in the right-hand side of Eq. (1) responsible for the interband absorption in the bottom GL, and using Eqs. (1), (2), and (6), we arrive at

$$\mathrm{Re}\ \sigma_\omega = \left(\frac{e^2}{4\hbar}\right)\left\{\frac{4k_BT\tau_B}{\pi\hbar(1+\omega^2\tau_B^2)}\ln\left[1+\exp\left(\frac{\varepsilon_F^B}{k_BT}\right)\right] + \frac{8k_BT\tau}{\pi\hbar(1+\omega^2\tau^2)}\sum_{k=1}^{K}\ln\left[1+\exp\left(\frac{\varepsilon_F^{(k)}}{k_BT}\right)\right] + \sum_{k=1}^{K}\tanh\left(\frac{\hbar\omega-2\varepsilon_F^{(k)}}{4k_BT}\right)\right\}. \tag{7}$$

The first two terms in the right-hand side of Eq. (7) describe the intraband (Drude) absorption of terahertz radiation in all GLs, whereas the third term is associated with the interband transitions. When the latter is negative, i.e., when the interband emission prevails the interband absorption, the quantity $\mathrm{Re}\ \sigma_\omega$ as a function of ω exhibits a minimum. At a strong optical pumping when the quantities $\varepsilon_F^{(k)}$ are sufficiently large, $\mathrm{Re}\ \sigma_\omega < 0$ in this minimum as well as in a certain range of frequencies $\omega_{\min} < \omega < \omega_{\max}$. Here $\omega_{\min}$ and $\omega_{\max}$ are the frequencies at which $\mathrm{Re}\ \sigma_\omega = 0$; they are determined by τ_B, τ, and ε_F^T (i.e., by the intensity of the incident optical pumping radiation).

Since in the MGL structure in question $\varepsilon_F^B \gg k_BT$, considering such frequencies that $\omega^2\tau_B^2$, $\omega^2\tau^2 \gg 1$, one can reduce Eq. (7) to the following:

$$\mathrm{Re}\ \sigma_\omega = \left(\frac{e^2}{4\hbar}\right)\left\{\frac{4\varepsilon_F^B}{\pi\hbar\omega^2\tau_B} + \frac{8k_BT}{\pi\hbar\omega^2\tau}\sum_{k=1}^{K}\ln\left[1+\exp\left(\frac{\varepsilon_F^{(k)}}{k_BT}\right)\right] + \sum_{k=1}^{K}\tanh\left(\frac{\hbar\omega-2\varepsilon_F^{(k)}}{4k_BT}\right)\right\}. \tag{8}$$

Under sufficiently strong optical pumping when $\varepsilon_F^{(k)} \gg \hbar\omega$, k_BT, and, consequently, $\tanh[(\hbar\omega - 2\varepsilon_F^{(k)})/4k_BT] \simeq -1$, setting $\Sigma_{k=1}^{K}\varepsilon_F^{(k)} \simeq K^*\varepsilon_F^T$, where $K^* < K$, from Eq. (8) one obtains

$$\mathrm{Re}\ \sigma_\omega\left(\frac{4\hbar}{e^2}\right) \simeq \frac{4}{\pi\hbar\omega^2}\left(\frac{\varepsilon_F^B}{\tau_B} + \frac{2K^*\varepsilon_F^T}{\tau}\right) - K. \tag{9}$$

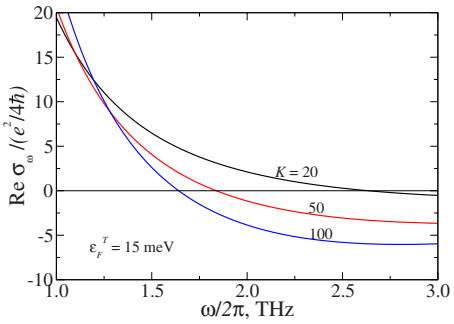

FIG. 2. (Color online) Frequency dependences of the real part of dynamic conductivity $\mathrm{Re}\ \sigma_\omega$ normalized by quantity $e^2/4\hbar$ for MGL structures with different number of GLs K at modest pumping ($\varepsilon_F^T = 15$ meV).

IV. FREQUENCY CHARACTERISTICS OF DYNAMIC CONDUCTIVITY

Figures 2 and 3 show the frequency dependences of $\mathrm{Re}\ \sigma_\omega$ normalized by $e^2/4\hbar$ calculated for MGL structures with different K at different values of ε_F^T (i.e., different optical pumping intensities) using Eqs. (1), (2), (5), and (6) or Eqs. (5) and (7). We set $\varepsilon_F^B = 400$ meV,[8] $\hbar\Omega = 920$ meV, $T = 300$ K, $\tau_B = 1$ ps, $\tau = 10$ ps, and $\gamma = 1/4$. As seen from Figs. 2 and 3, $\mathrm{Re}\ \sigma_\omega$ can be negative in the frequency range $\omega > \omega_{\min}$ with $\omega_{\min}$ decreasing with increasing quasi-Fermi energy ε_F^T in the topmost GL, i.e., with increasing optical pumping intensity (see below). In the MGL structures with $K = 50$–100 at $\varepsilon_F^T = 30$–50 meV, one has $\omega_{\min}/2\pi \gtrsim 1$ THz (see Figs. 3 and 4). As follows from the inset on upper panel in Fig. 3, the quantities $\varepsilon_F^{(k)}$ are not too small in comparison with ε_F^T even in GLs with the indices $k \ll K$, i.e., in GLs near the MGL structure bottom. This implies that the pumping of such near bottom GLs is effective even in the MGL structures with $K \sim 100$. The quantity $\mathrm{Re}\ \sigma_\omega$ as a function of ω exhibits a minimum (see the inset on lower panel in Fig. 3). The sign of $\mathrm{Re}\ \sigma_\omega$ becomes positive at $\omega > \omega_{\max}$, where $\omega_{\max}$

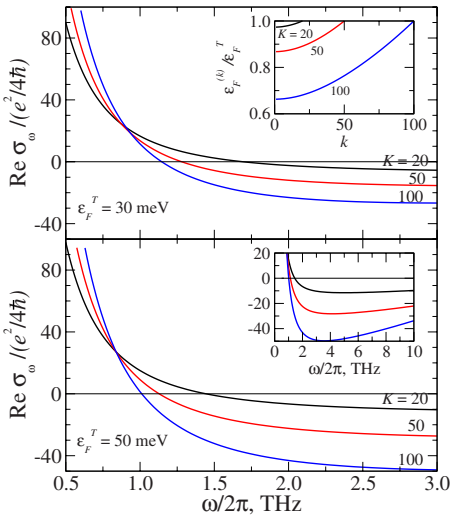

FIG. 3. (Color online) Frequency dependences of the real part of dynamic conductivity $\mathrm{Re}\ \sigma_\omega$ normalized by quantity $e^2/4\hbar$ for MGL structures with different number of GLs K at $\varepsilon_F^T = 30$ and 50 meV. The inset on the upper panel shows how the GL population varies with the GL index k, whereas the inset on the lower panel demonstrates the dependences but in a wider range of frequencies.

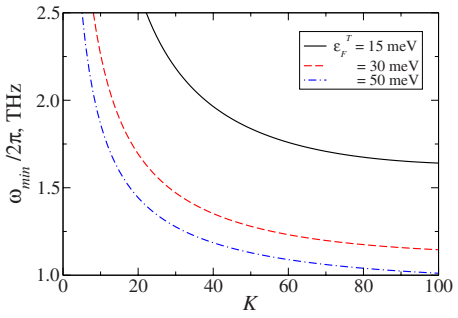

FIG. 4. (Color online) Dependences of min σ_ω on number of GLs.

is rather large (more than 10 THz). The MGL structures with a larger number K of GLs at stronger pumping exhibit smaller $\omega_{\min}$ and deeper minima Re σ_ω. This is confirmed also by Fig. 5.

V. ROLE OF THE BOTTOM GL

The highly conducting bottom GL, whose existence is associated with the intrinsic features of the MGL structure growth, plays the negative role. This is mainly because it results in a marked absorption (due to the Drude mechanism) of the terahertz radiation emitted by other GLs. Since such an absorption increases with decreasing frequency, the achievement of the negative dynamic conductivity in the MGL structures with shorter momentum relaxation times τ_B and τ even at higher frequencies is significantly complicated by the Drude absorption. This is demonstrated by Fig. 6 (upper panel). In contrast, a decrease in the Fermi energy ε_F^B and the electron density in the bottom GL, of course, might significantly promote the achievement of negative dynamic conductivity in a wide frequency range, particularly at relatively low frequencies (compare the frequency dependences on upper and lower panels in Fig. 6). In this regard, the MGL structures with GLs exhibiting a long relaxation time τ (like that found in Ref. 10) but with a lowered electron density in the bottom GL or without the bottom layer appears to be much more preferable. Such MGL structures can be fabricated using chemical/mechanical reactions and transferred substrate techniques (chemically etching the substrate and the highly conducting bottom GL (Ref. 12) or mechanically peeling the upper GLs, then transferring the upper portion of the MGL structure on a Si or equivalent transparent substrate). The calculation of Re σ_ω for this MGL structure can

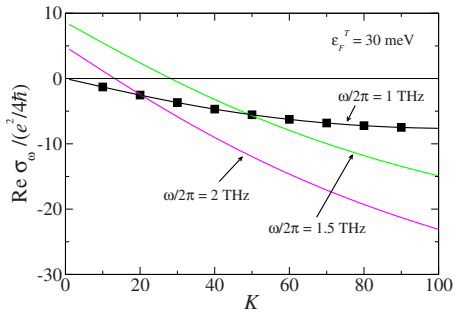

FIG. 5. (Color online) Real part of the normalized dynamic conductivity as a function of the number of GLs for different frequencies. The line with markers corresponds to a MGL structure without the bottom GL.

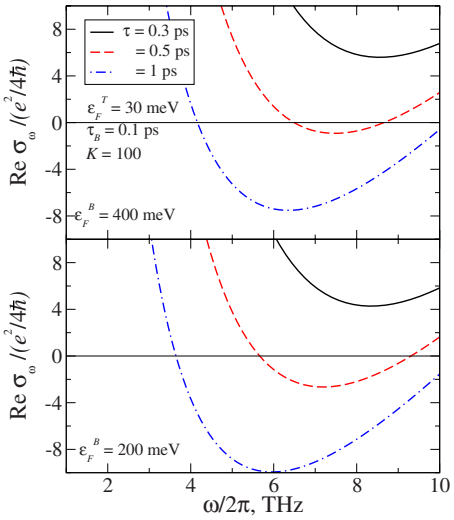

FIG. 6. (Color online) Real part of the normalized dynamic conductivity vs frequency calculated for MGL structures with τ_B=0.1 ps and different τ and ε_F^B.

be carried out by omitting the term Re σ_ω in Eq. (6). The pertinent results are shown in Fig. 5 (see the marked line) and Fig. 7. Here, as in Fig. 3, we assumed that $\hbar\omega$ =920 meV, T=300 K, τ_B=1 ps, and τ=10 ps. The obtained frequency dependences are qualitatively similar to those shown in Figs. 2 and 3. However the dependences for the MGL structures without the bottom layer exhibit a marked shift toward lower frequencies. In particular, as follows from Figs. 5 and 7, Re σ_ω can be negative even at $\omega/2\pi \lesssim 1$ THz (at chosen values of ε_F^T).

VI. CONDITION OF LASING

To achieve lasing in the MGL structures under consideration, the following condition should be satisfied:[7]

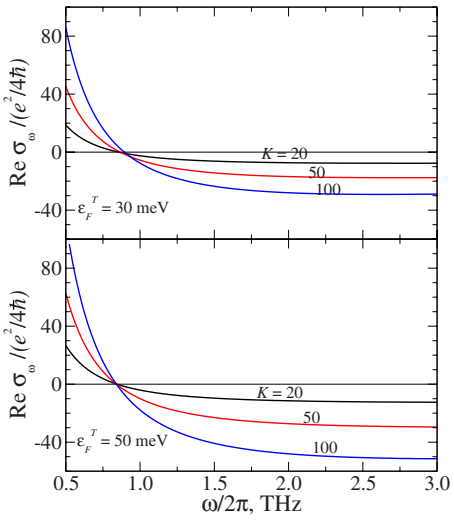

FIG. 7. (Color online) Real part of the normalized dynamic conductivity vs frequency calculated for MGL structures with different numbers of GLs and without bottom GL.

$$\frac{8\pi}{c}|\mathrm{Re}\ \sigma_\omega|E_t^2 > (1-r_1)E_1^2 + (1-r_2)E_2^2 + (a/R)^2E_1^2 + E_S^2. \tag{10}$$

Here, E_t, E_1, and E_2 are maximum amplitudes of the terahertz electric field $E=E(z)$ at the MGL structure (placed at the distance t from the bottom mirror, where t is the thickness of the substrate), and near the pertinent mirror, respectively, $E_S^2=(\alpha_S n_S/2)\int_0^t E^2 dz$, α_S and n_S are the absorption coefficient of THz radiation in the substrate (SiC or Si) and real part of its refraction index, r_1 and r_2 are the reflection coefficients of THz radiation from the mirrors, and a/R is the ratio of the diameters of the output hole a and the mirror R. In deriving inequality (10), we neglected the finiteness of the MGL thickness (in comparison with t and the THz wavelength) and disregarded the diffraction losses. For simplicity, one can set $E_t^2 \sim E_1^2 \sim E_2^2$ and $E_S^2 \sim (t\alpha_S n_S/2)E_2^2$, disregarding, in particular, partial reflection of THz radiation from the bottom GL. In this case, inequality (10) can be presented as

$$\frac{8\pi}{c}|\mathrm{Re}\ \sigma_\omega| > (1-r_1) + (1-r_2) + (a/R)^2 + t\alpha_S n_S/2 = L. \tag{11}$$

Assuming that $r_1=r_2=0.99$, $(a/R)=0.1$, $\alpha_S \simeq 2-4\ \mathrm{cm}^{-1}$, $n_S \simeq 3$,[13] and $t=50\ \mu\mathrm{m}$, for L one obtains $L=0.06-0.09$. However, as follows from Fig. 5, the quantity $(8\pi/c)|\mathrm{Re}\ \sigma_\omega|$ for a MGL structure with $K=100$ at $\omega/2\pi=1.5$ THz at $\varepsilon_F^T=30$ meV is about $12\beta \simeq 0.275$. At $\omega/2\pi=1.0$ THz but for the structure without the bottom GL (see the line with markers in Fig. 5), one obtains $(8\pi/c)|\mathrm{Re}\ \sigma_\omega| \simeq 0.345$. These values of $(8\pi/c)|\mathrm{Re}\ \sigma_\omega|$ well exceed the above value of L (in contrast with the structures with two GLs,[7] for which the minimization of the losses is crucial). At the elevated frequencies, the ratio $(8\pi/c)|\mathrm{Re}\ \sigma_\omega|/L$ can be even much larger.

Considering that the electron (hole) density Σ^T in the topmost GL

$$\Sigma^T = \frac{2}{\pi\hbar^2}\int_0^\infty \frac{dpp}{1+\exp[(v_F p - \varepsilon_F^T)/k_B T]}$$

at $\varepsilon_F^T=30$ meV at $T=300$ K, we obtain $\Sigma^T \simeq 2\times 10^{11}\ \mathrm{cm}^{-2}$. Such a value (and higher) of the photogenerated electron and hole density is achievable experimentally (see, for instance, Ref. 14). Assuming that $K=100$, $\hbar\Omega=920$ meV, and the recombination time $\tau_R \simeq 20$ ps at $T=300$ K and $\Sigma^T \simeq 2\times 10^{11}\ \mathrm{cm}^{-2}$,[15] for the pertinent optical pumping power we obtain $I_\Omega \simeq 6.4\times 10^4\ \mathrm{W/cm}^2$. One needs to point out that this value of I_Ω is much larger than the threshold of lasing at a certain frequency ($\omega_{\min} < \omega < \omega_{\max}$). At $T=100$ K, the recombination time (due to optical phonon emission) is much longer,[15] hence, the electron and hole densities in question can be achieved at much weaker optical pumping.

In the regime sufficiently beyond the threshold of lasing, when the stimulated radiative recombination becomes dominant, the pumping efficiency is determined just by the ratio of the energy of the emitted terahertz photons $\hbar\omega$ and the energy of optical photons $\hbar\Omega$, $\eta=\omega/\Omega$. However, the nonradiative recombination mechanisms can markedly decrease η. In the regime in question, the maximum output terahertz power can be estimated as $\max P_\omega \simeq \pi R^2(\omega/\Omega)I_\Omega$. For example, at $\hbar\Omega=920$ meV, $\hbar\omega/2\pi=5.9$ meV ($\omega/2\pi \simeq 1.5$ THz), $2R=0.1$ cm, and $I_\Omega=3\times 10^4\ \mathrm{W/cm}^2$, one obtains $\max P_\omega \simeq 1.5$ W.

VII. CONCLUSIONS

We studied real part of the dynamic conductivity of a MGL structure with a stack of GLs and a highly conducting bottom GL on SiC substrate pumped by optical radiation. It was shown that the negative dynamic conductivity in the MGL structures under consideration with sufficiently large number K of perfect upper GLs can be achieved even at room temperature provided the optical pumping is sufficiently strong. Due to large K, the absolute value of $\mathrm{Re}\ \sigma_\omega$ in its minimum can significantly exceed the characteristic value of conductivity $e^2/4\hbar$. Thus, the MGL structures can serve as active media of terahertz lasers. This can markedly liberate the requirement for the quality of the terahertz laser resonant cavity. An increase in τ_B and τ promotes widening of the frequency range where $\mathrm{Re}\ \sigma_\omega < 0$, particularly, at the low end of this range. This opens up the prospects of terahertz lasing with $\omega/2\pi \sim 1$ THz even at room temperature. The main obstacle appears to be the necessity of sufficiently long relaxation times τ_B and τ in GLs with rather high electron and hole densities: $\Sigma > 10^{11}\ \mathrm{cm}^{-2}$. Since the electron-hole recombination at the temperatures and densities under consideration might be attributed to the optical phonon emission,[15] the optical pumping intensity required for terahertz lasing can be markedly lowered (by orders of magnitudes) with decreasing temperature. The conditions of lasing in the MGL structures without the bottom GL are particularly liberal.

ACKNOWLEDGMENTS

One of the authors (V.R.) is grateful to M. Orlita and F.T. Vasko for useful discussions and information. This work was supported by the Japan Science and Technology Agency, CREST, Japan.

APPENDIX: RECOMBINATION

The rate of radiative recombination in the degenerate electron-hole system in the topmost GL due to spontaneous emission of photons at $\varepsilon_F^T \gg k_B T$ can be calculated using the following formula:[6,16]

$$R_r \simeq \frac{2v_r}{\pi\hbar^3}\int_0^{\varepsilon_F^T/v_F} dpp^2 = \frac{2v_r(\varepsilon_F^T)^3}{3\pi\hbar^3 v_F^3} \propto (\varepsilon_F^T)^3. \tag{A1}$$

Here $v_r=\sqrt{\varkappa}(8e^2/3\hbar c)(v_F/c)^2 v_F$ and $\varkappa$ is the dielectric constant $p_F=\varepsilon_F^T/v_F$.

The rate of the electron-hole recombination associated with emission of optical phonons can be described the following equation:[14]

$$R_{ph} \propto \int_0^{\hbar\omega_0/v_F} \frac{dpp(\hbar\omega_0/v_F - p)}{\left[1+\exp\left(\frac{v_F p - \varepsilon_F^T}{k_B T}\right)\right]\left[1+\exp\left(\frac{\hbar\omega_0 - v_F p - \varepsilon_F^T}{k_B T}\right)\right]} \propto \exp\left(\frac{2\varepsilon_F^T - \hbar\omega_0}{k_B T}\right). \tag{A2}$$

Equalizing R_r^T and the rate of generation of electrons and holes by the optical pumping radiation G_Ω^T and the recombination rate, and considering Eqs. (A1) and (A2), one can find that $\varepsilon_F^T \propto (G_\Omega^T)^{1/3}$ and $\varepsilon_F^T \propto \ln(G_\Omega^T)$, respectively. The radiative interband transitions stimulated by the thermal photons can also contribute to the recombination rate[6,16] as well as the processes of electron-hole interaction in the presence of disorder. These processes provide different dependences of the recombination rate on the quasi-Fermi energy. Due to this, calculating the dependence of the latter in different GLs on the optical pumping intensity, we put, for definiteness, $\varepsilon_F^T \propto (G_\Omega^T)^\gamma$ with $\gamma = 1/4$. Such a dependence is less steep than that for the spontaneous radiative recombination and somewhat steeper than in the case of optical phonon recombination. The variation in parameter γ leads to some change in the $\varepsilon_F^{(k)} - k$ dependence, but it should not affect the main obtained results.

[1]C. Berger, Z. Song, T. Li, X. Li, A. Y. Ogbazhi, R. Feng, Z. Dai, A. N. Marchenkov, E. H. Conrad, P. N. First, and W. A. de Heer, J. Phys. Chem. **108**, 19912 (2004).
[2]K. S. Novoselov, A. K. Geim, S. V. Morozov, D. Jiang, M. I. Katsnelson, I. V. Grigorieva, S. V. Dubonos, and A. A. Firsov, Nature (London) **438**, 197 (2005).
[3]V. Ryzhii, M. Ryzhii, and T. Otsuji, J. Appl. Phys. **101**, 083114 (2007).
[4]M. Ryzhii and V. Ryzhii, Jpn. J. Appl. Phys., Part 2 **46**, L151 (2007).
[5]F. Rana, IEEE Trans. Nanotechnol. **7**, 91 (2008).
[6]A. Satou, F. T. Vasko, and V. Ryzhii, Phys. Rev. B **78**, 115431 (2008).
[7]A. A. Dubinov, V. Ya. Aleshkin, M. Ryzhii, T. Otsuji, and V. Ryzhii, Appl. Phys. Express **2**, 092301 (2009).
[8]F. Varchon, R. Feng, J. Hass, X. Li, B. Ngoc Nguyen, C. Naud, P. Mallet, J.-Y. Veuillen, C. Berger, E. H. Conrad, and L. Magaud, Phys. Rev. Lett. **99**, 126805 (2007).
[9]M. Orlita, C. Faugeras, P. Plochocka, P. Neugebauer, G. Martinez, D. K. Maude, A.-L. Barra, M. Sprinkle, C. Berger, W. A. de Heer, and M. Potemski, Phys. Rev. Lett. **101**, 267601 (2008).
[10]P. Neugebauer, M. Orlita, C. Faugeras, A.-L. Barra, and M. Potemski, Phys. Rev. Lett. **103**, 136403 (2009).
[11]L. A. Falkovsky and A. A. Varlamov, Eur. Phys. J. B **56**, 281 (2007).
[12]A. Bostwick, T. Ohta, T. Seyller, K. Horn, and E. Rotenberg, Nat. Phys. **3**, 36 (2007).
[13]J. H. Strait, P. A. George, J. M. Dawlaty, S. Shivaraman, M. Chanrashekhar, F. Rana, and M. G. Spencer, Appl. Phys. Lett. **95**, 051912 (2009).
[14]J. M. Dawlaty, S. Shivaraman, M. Chandrashekhar, F. Rana, and M. G. Spencer, Appl. Phys. Lett. **92**, 042116 (2008).
[15]F. Rana, P. A. George, J. H. Strait, S. Shivaraman, M. Chanrashekhar, and M. G. Spencer, Phys. Rev. B **79**, 115447 (2009).
[16]F. T. Vasko and V. Ryzhii, Phys. Rev. B **77**, 195433 (2008).